Functional interactions between BLM and XRCC3 in the cell

Makoto Otsuki,[1] Masayuki Seki,[1] Eri Inoue,[1] Akari Yoshimura,[1] Genta Kato,[1] Saki Yamanouchi,[1] Yoh-ichi Kawabe,[1] Shusuke Tada,[1] Akira Shinohara,[2] Jun-ichiro Komura,[5] Tetsuya Ono,[5] Shunichi Takeda,[3] Yutaka Ishii,[4] and Takemi Enomoto[1,6]

[1]Molecular Cell Biology Laboratory, Graduate School of Pharmaceutical Science, Tohoku University, Sendai 980-8578, Japan
[2]Institute for Protein Research, Graduate School of Science, Osaka University, Suita, Osaka 565-0871, Japan
[3]Department of Radiation Genetics, Kyoto University Graduate School of Medicine, Kyoto 606-8501, Japan
[4]Shujitsu University, School of Pharmacy, Nishigawara, Okayama 703-8516, Japan
[5]Department of Cell Biology, Graduate School of Medicine, Tohoku University, Aoba-ku, Sendai, 980-8575 Japan
[6]21st Century Centers of Excellence Program, Comprehensive Research and Education Center for Planning of Drug development and Clinical Evaluation, Tohoku University, Sendai, Miyagi 980-8578, Japan

Bloom's syndrome (BS), which is caused by mutations in the *BLM* gene, is characterized by a predisposition to a wide variety of cancers. BS cells exhibit elevated frequencies of sister chromatid exchanges (SCEs), interchanges between homologous chromosomes (mitotic chiasmata), and sensitivity to several DNA-damaging agents. To address the mechanism that confers these phenotypes in BS cells, we characterize a series of double and triple mutants with mutations in *BLM* and in other genes involved in repair pathways. We found that XRCC3 activity generates substrates that cause the elevated SCE in *blm* cells and that BLM with DNA topoisomerase IIIα suppresses the formation of SCE. In addition, XRCC3 activity also generates the ultraviolet (UV)- and methyl methanesulfonate (MMS)–induced mitotic chiasmata. Moreover, disruption of *XRCC3* suppresses MMS and UV sensitivity and the MMS- and UV-induced chromosomal aberrations of *blm* cells, indicating that BLM acts downstream of XRCC3.

Introduction

Bloom's syndrome (BS) is a rare autosomal recessive disease characterized by a predisposition to a wide variety of cancers (German 1993). The responsible gene product, BLM, is a member of the highly conserved RecQ family of DNA helicases (Ellis et al., 1995). Cells derived from BS patients exhibit elevated frequencies of sister chromatid exchanges (SCEs), chromosomal breaks, interchanges between homologous chromosomes, and sensitivity to several DNA-damaging agents. The single RecQ helicase homologues of *Saccharomyces cerevisiae* (Sgs1; Gangloff et al. 1994) and *Schizosaccharomyces pombe* (Rqh1; Stewart et al., 1997) play critical roles in the maintenance of genomic stability. In human cells, five genes encoding RecQ helicase homologues have been identified, and defects in two of them, *WRN* and *RTS*, cause Werner's syndrome and Rothmund-Thomson syndrome, respectively, which are disorders associated with genomic instability (Yu et al., 1996; Kitao et al., 1999).

Correspondence to M. Seki: seki@mail.pharm.tohoku.ac.jp

Abbreviations used in this paper: BS, Bloom's syndrome; HJ, Holliday junction; *hXRCC3*, human *XRCC3*; MMS, methyl methanesulfonate; SCE, sister chromatid exchange; TOP3α, topoisomerase IIIα.

The online version of this article contains supplemental material.

Biochemical analyses indicated that BLM demonstrates G4 DNA unwinding, branch migration, and canonical DNA helicase activity (Bachrati and Hickson, 2003). More importantly, BLM with DNA topoisomerase IIIα (TOP3α) was shown to resolve double Holliday junctions (HJs) to yield noncrossover products (Wu and Hickson, 2003). BLM interacts physically with several proteins involved in various aspects of DNA metabolism, such as RAD51 and WRN (Wu et al., 2001; von Kobbe et al., 2002). In addition, BLM is a component of the BRCA1-associated genome surveillance complex (Y. Wang et al., 2000), which contains BRCA1, ATM, MRE11, RAD50, NBS1, MSH2, MSH6, and RFC, and a complex containing the five Fanconi anemia complementation proteins (FANCA, FANCG, FANCC, FANCE, and FANCF), RPA, TOP3α, and BLAP75 (Meetei et al., 2003; Yin et al., 2005). BLAP75 was recently shown to stimulate the dissolution of double HJs by BLM and TOP3α (Raynard et al., 2006; Wu et al., 2006).

Despite the accumulation of biochemical data on the activities and binding partners of BLM, little is known about its biological functions. Recently, we have reported a possible involvement of BLM and TOP3α in the dissolution of sister chromatids during the late stage of DNA replication using corresponding

The Journal of Cell Biology, Vol. 179, No. 1, October 8, 2007 53–63
http://www.jcb.org/cgi/doi/10.1083/jcb.200702183

gene-disrupted chicken DT40 cells (Seki et al., 2006a). However, in BS cells, the molecular basis of the elevated frequencies of SCE, interchanges between homologous chromosomes, and their sensitivity to several DNA-damaging agents is not well understood. To address the mechanism that confers these BS cell phenotypes and to understand the functions of BLM in the cell, we used chicken DT40 cells to establish and characterize double and triple *blm* mutants bearing mutations in other genes involved in various repair pathways, including homologous recombination (*XRCC3*, *RAD52*, and *RAD54*). Based on our data, we discuss BLM function and propose an error-free lesion bypass mechanism that involves XRCC3 and BLM.

Results

Generation of various BLM-deficient and XRCC3-deficient cell lines

To investigate the function of BLM under DNA damage–inducing conditions, we generated double and triple mutants of *BLM* bearing mutations in genes of the *RAD52* epistasis group (*RAD52*, *RAD54*, and *XRCC3*) that are relevant for homologous recombination, and in genes involved in postreplication repair (*RAD18*) and nonhomologous end-joining (*KU70*) using the chicken B cell line DT40 (Bezzubova et al., 1997; Takata et al., 1998, 2001; Yamaguchi-Iwai et al., 1998; Yamashita et al., 2002). We generated five mutants with *XRCC* gene–disrupted (*xrcc3*) cells containing human *XRCC3* (*hXRCC3*) and *EGFP* transgenes, which can be deleted by activating the Cre recombinase with 4-hydroxy tamoxifen (Ishiai et al., 2004). Although growth of *hXRCC3*-complemented *xrcc3* cells was slightly slower than that of wild-type cells, the sensitivities of the cells to methyl methanesulfonate (MMS) and UV were indistinguishable from those of wild-type cells (unpublished data). Thus, we considered *hXRCC3*-complemented *xrcc3* cells to be equivalent to wild-type cells. A scheme for the systematic generation of the various double and triple mutants from *xrcc3+hXRCC3* ("wild-type") cells is shown in Fig. 1 A. Gene disruption was confirmed by RT-PCR (Fig. 1 B) and genomic PCR (not depicted). Generation of *rad52/blm*, *ku70/blm*, and *rad18/blm* cells is shown in Fig. 1 C and described in Materials and methods.

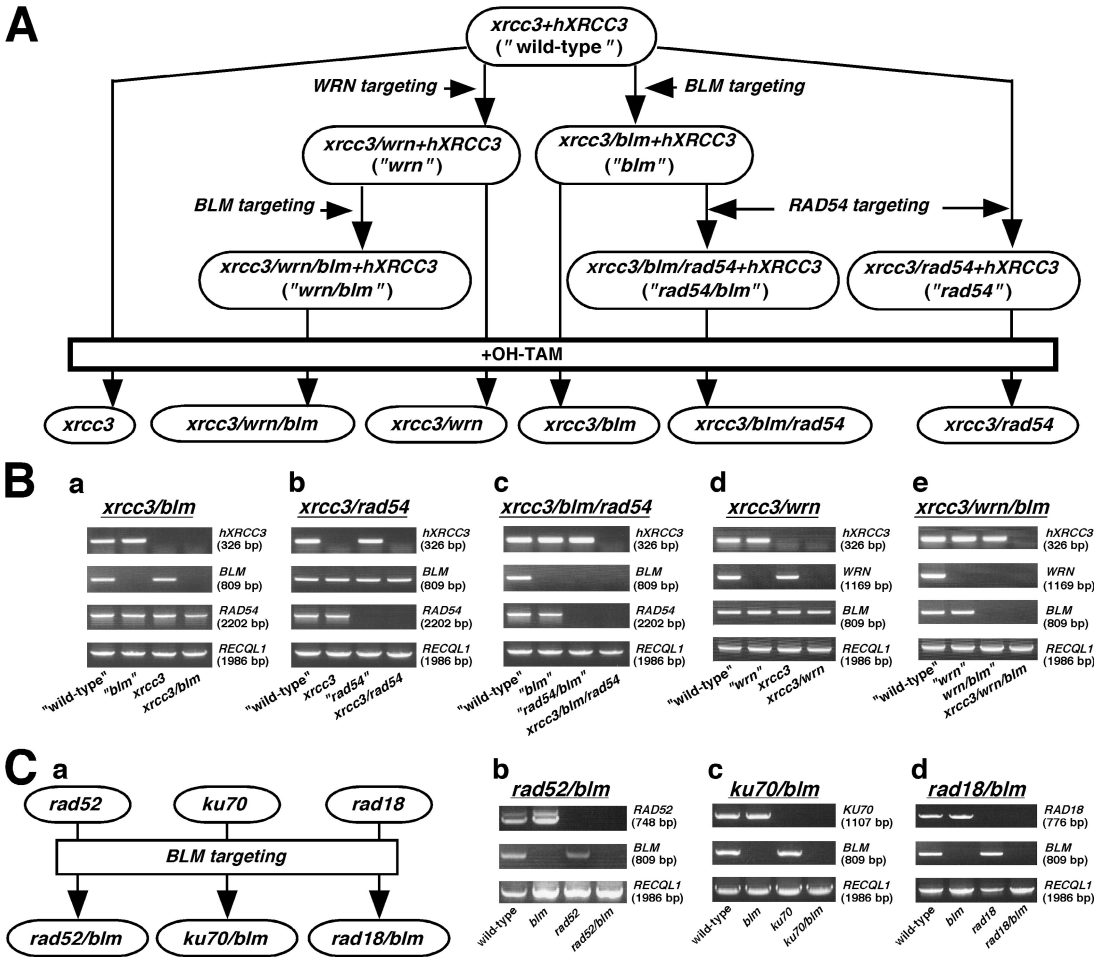

Figure 1. **Generation of double and triple mutants of *BLM* with mutations in other genes involved in DNA repair pathways.** (A) Schematic representation of the generation of several mutants in a conditional *xrcc3* background. (B) RT-PCR analysis of total RNA from the indicated mutants in the conditional *xrcc3* background. (a–c) Each mutant cell line was examined for the expression of *hXRCC3*, *BLM*, *RAD54*, and *RECQL1* mRNA. *RECQL1* was amplified as a control. (d and e) Each mutant cell line was examined for the expression of *hXRCC3*, *WRN*, *BLM*, and *RECQL1* mRNA. (C) Disruption of *BLM* in the indicated single gene mutants. (a) Schematic representation of the generation of mutants. (b–d) RT-PCR analysis of total RNA from the indicated mutants.

Elevated SCE in *blm* cells depends on XRCC3

A characteristic feature of BS cells is a high incidence of SCE. A possible explanation for this property is that BLM with TOP3α dissolves double HJs in a manner that does not produce crossovers, and that the BLM defect results in crossovers that are detected as SCE. Double HJs are formed by the activities of proteins involved in homologous recombination such as RAD51 (Ira et al., 2003; Wu and Hickson, 2003). Thus, we investigated the frequency of SCE in relevant mutant cells. As shown in Fig. 2 A, the SCE frequency in *xrcc3* cells was lower than in *xrcc3+hXRCC3* cells, and the elevated SCE frequency in *xrcc3/blm+hXRCC3* ("*blm*") cells was greatly reduced by deletion of *hXRCC3* (Fig. 2 A, bottom). We previously reported that disruption of *RAD54* considerably reduces the frequency of SCE in *blm* cells (W. Wang et al., 2000). As expected, the *xrcc3/blm/rad54+hXRCC3* ("*blm/rad54*") cells generated in this study showed a lower SCE frequency than *xrcc3/blm+hXRCC3* cells (Fig. 2 B). In contrast, disruption of *RAD52* did not affect the increased frequency of SCE in *blm* cells (Fig. 2 C).

We also examined the functional relationship between BLM and TOP3α in the suppression of SCE. As TOP3α-depleted cells exhibit lethality, we previously generated *top3α* and *top3α/blm* cells carrying a mouse *Top3α* transgene placed under the control of the doxycyclin-repressible promoter (Seki et al., 2006a). The *top3α* cells ceased to grow within 3 d after the addition of doxycyclin, and they showed an increase in SCE frequency 2 d after the treatment, as similarly observed for *blm* cells (Fig. 2 D). Moreover, the SCE frequency in *top3α/blm* cells 2 d after doxycyclin addition was almost the same as that of *blm* cells, indicating that TOP3α functions with BLM to suppress the formation of SCE. Notably, disruption of *TOP3β* did not increase the SCE frequency (Fig. 2 E).

BLM and XRCC3 belong to the same DNA-repair or damage-tolerance pathway

To identify the pathway in which BLM functions under DNA damage–inducing conditions, we performed colony survival assays of various mutant cells in the presence of MMS. Double mutant *ku70/blm* and *rad18/blm* cells were more sensitive to MMS than either single mutant (Fig. 3 A). The same tendency was also seen in *rad52/blm* cells.

Interestingly, the MMS sensitivity of *xrcc3/blm+hXRCC3* cells was partially suppressed by disruption of *XRCC3* (Figs. 3 B, a,

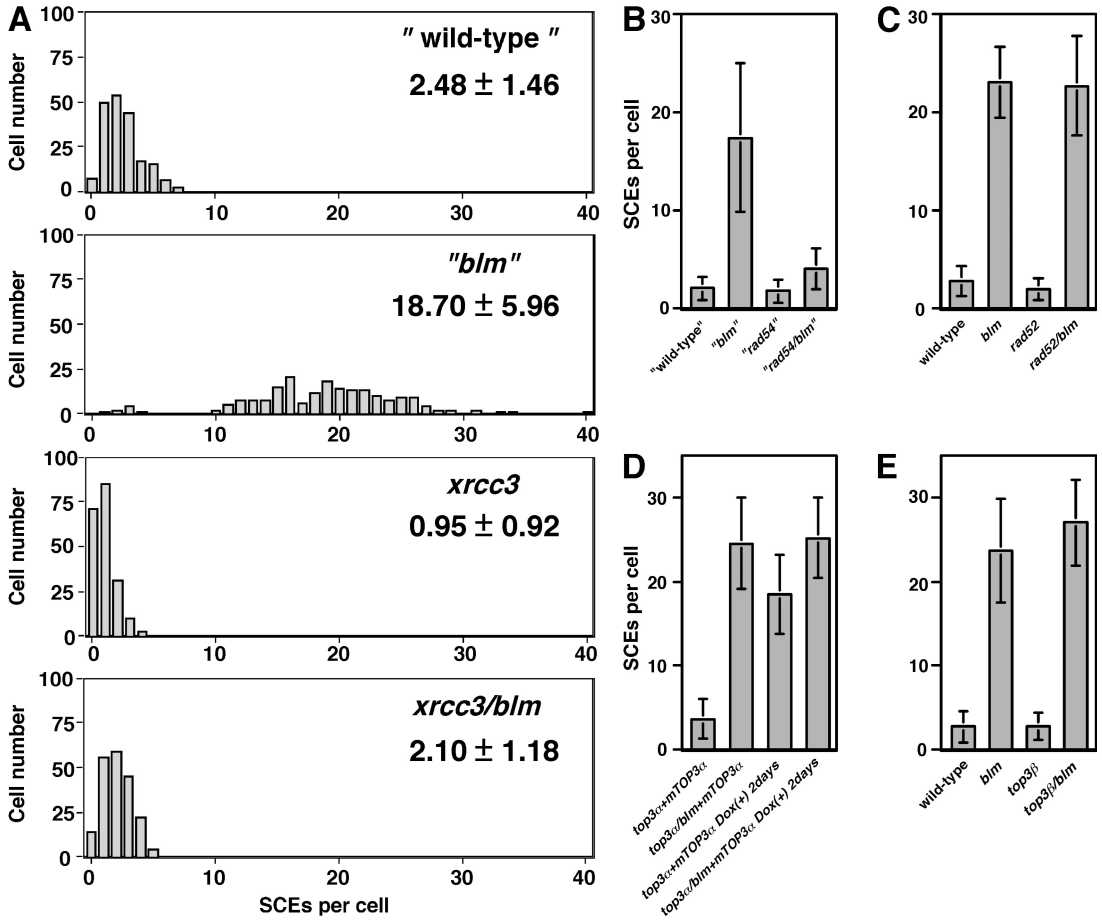

Figure 2. **Spontaneous SCE levels of various mutants.** (A) SCE levels of *xrcc3+hXRCC3* ("wild-type"), *xrcc3/blm+hXRCC3* ("*blm*"), *xrcc3*, and *xrcc3/blm* cells. Numbers represent means and SDs of scores from two hundred metaphase cells. (B) SCE levels of *xrcc3+hXRCC3*, *xrcc3/blm+hXRCC3*, *xrcc3/rad54+hXRCC3* ("*rad54*"), and *xrcc3/blm/rad54+hXRCC3* ("*blm/rad54*") cells. (C) SCE levels of wild-type, *blm*, *rad52*, and *rad52/blm* cells. (D) SCE levels of *top3α* and *top3α/blm* cells in a conditional *top3α* background. The expression of mouse *Top3α* is suppressed by doxycyclin. (E) SCE levels of wild-type, *blm*, *top3β*, and *top3β/blm* cells. The error bars show SD of scores from 100 metaphase cells.

and S1 A, available at http://www.jcb.org/cgi/content/full/jcb.200702183/DC1). All clones of *xrcc3/blm* cells derived from the same parental *xrcc3/blm+hXRCC3* cells showed almost the same sensitivity to MMS (unpublished data), which excluded the possibility that the suppression of MMS sensitivity was caused by mutations occurring during mutant isolation. Thus, BLM appears to function downstream of XRCC3 under damage-inducing conditions.

It has been reported that *wrn/blm* cells show synergistic or additive increases in sensitivity to genotoxic agents including MMS, compared with either single mutant (Imamura et al., 2002), suggesting that BLM and WRN perform nonoverlapping functions. The MMS sensitivity of *xrcc3/wrn* cells was higher than that of either single mutant (Fig. 3 B, b), suggesting that WRN functions independently of XRCC3 in response to MMS-induced damage. However, the MMS sensitivity of *xrcc3/wrn/blm* triple mutant cells was not higher than that of *xrcc3/wrn/blm+hXRCC3* ("*wrn/blm*") or *xrcc3/wrn* cells (Fig. 3 B, c), indicating that BLM and XRCC3 function in the same pathway, even in the *wrn* background.

In contrast to what we found for *XRCC3*, we previously observed that *blm/rad* cells show higher sensitivity to genotoxic agents, including MMS (W. Wang et al., 2000), compared with either single mutant. *xrcc/blm/rad54+hXRCC3* cells were similarly more MMS sensitive than either single mutant (Fig. 3 C, a). In *S. cerevisiae*, proteins belonging to the RAD52 epistasis group, such as RAD51, RAD54, RAD55, and RAD57, are involved in recombinational repair (Sung et al., 2000). Thus, it is possible that XRCC3, a RAD51 paralogue in higher eukaryotic cells, functions in a recombinational repair pathway involving RAD54. Therefore, we examined the MMS sensitivity of *xrcc3/rad54* and *xrcc3/blm/rad54* cells. The MMS sensitivity of the *xrcc3/rad54* cells was higher than that of either single mutant (Figs. 3 C, b, and S1 B), and the sensitivity of *xrcc3/blm/rad54* cells was almost

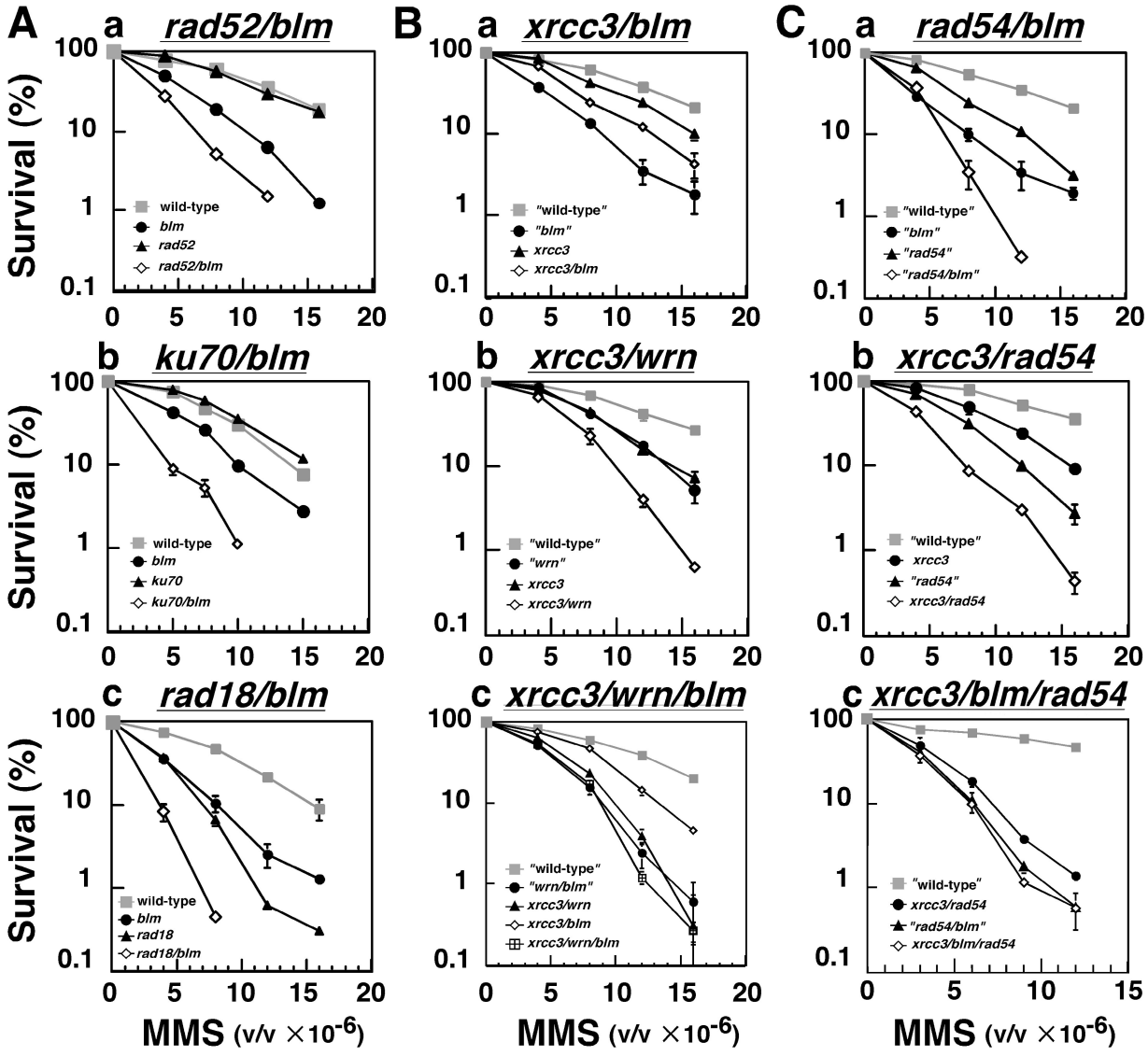

Figure 3. **Survival curves of mutant cells exposed to MMS.** (A–C) Cells were treated with the indicated concentrations of MMS. Colonies were counted after 7–14 d, and the percent survival was determined relative to the number of colonies of untreated cells. Representative data are shown. The error bars indicate SD. The differences in the duplicated data were often so minute that the SD was hidden by the symbols in the figures.

the same as that of *xrcc3/blm/rad54+hXRCC3* cells (Fig. 3 C, c). Thus, the genetic data obtained here are compatible with the notion that BLM and XRCC3 function in the same DNA repair or damage tolerance pathway after MMS treatment, but probably not in the canonical recombinational repair pathway.

To investigate the functional relationship between BLM and XRCC3, we examined RAD51 focus formation after exposure to MMS (unpublished data). After MMS treatment, an increase in the number of cells exhibiting RAD51 foci was observed in both *xrcc3/blm+hXRCC3* and *xrcc3+hXRCC3* cells. However, *xrcc3* and *xrcc3/blm* cells showed little increase in the number of RAD51 foci after MMS exposure. In contrast, MMS-induced RAD51 focus formation was observed in *rad52* and *rad52/blm* cells. These results indicated that RAD51 focus formation does not correlate with survival after exposure to MMS.

Chromosomal aberrations in *blm*, *xrcc3*, and *xrcc3/blm* cells induced by exposure to MMS

To understand the mechanism of the suppression of MMS sensitivity in *xrcc3/blm+hXRCC3* cells after disruption of *XRCC3*, we examined *xrcc3/blm*, *rad52/blm*, and related cell lines for a variety of chromosomal aberrations (the types of chromosome aberrations analyzed are presented in Fig. S2, A and B, available at http://www.jcb.org/cgi/content/full/jcb.200702183/DC1). As shown in Fig. 4 A, the number of chromosomal aberrations increased 12 h after exposure to MMS in all cells examined; *xrcc3/blm+hXRCC3* cells had a higher number of chromosome aberrations than *xrcc3+hXRCC3* and *xrcc3* cells, and the defect in *xrcc3/blm+hXRCC3* cells was suppressed by deletion of *hXRCC3*.

In contrast, a slight increase in chromosomal aberrations was observed in *rad52/blm* cells compared with either single mutant after exposure to MMS (Fig. 4 B), indicating that disruption of *XRCC3* but not *RAD52* specifically suppresses the defect in *blm* cells.

Elevation of MMS-induced mitotic chiasmata in *blm* cells

We next focused our attention on chromatid exchanges. Although we observed chromatid exchanges between nonhomologous chromosomes or different regions of homologous chromosomes (Fig. S3 A, available at http://www.jcb.org/cgi/content/full/jcb.200702183/DC1), the majority of chromatid exchanges observed after exposure to MMS involved homologous chromosomes, which is a typical feature of chicken DT40 cells (Fig. 4 C). This type of chromosomal aberration is called a mitotic chiasma because it resembles the chiasma structure seen in meiosis. A slight increase of mitotic chiasmata was observed in *xrcc3/blm+hXRCC3* cells compared with *xrcc3+hXRCC3* cells (Fig. 4 D, a). This phenotype is reminiscent of the increased interchanges between homologous chromosomes in BS cells (Chaganti et al., 1974). As shown in Fig. 4 D, MMS-induced mitotic chiasmata in *xrcc3+hXRCC3* and *xrcc3/blm+hXRCC3* cells were almost completely suppressed by deletion of *hXRCC3* (Fig. 4 D, a), whereas disruption of *RAD52* had no effect on the formation of mitotic chiasmata (b). In chromosomes forming mitotic chiasmata, it is generally held that the events of homologous recombination, but not the separation of the recombinant chromosomes linked by sister chromatid cohesion, have been completed (Fig. S3 B; Huttner and Ruddle, 1976; Therman and Kuhn, 1981). If this were the case, RAD54 would also be likely to be required for the formation of mitotic chiasmata. Indeed, RAD54 was required for mitotic chiasma formation in the presence or absence of BLM (unpublished data).

UV sensitivity and increased chromosomal aberrations of *blm* cells are suppressed by disruption of *XRCC3*

As described in the previous section, we analyzed *blm* cells and *blm*-related double mutant cells after exposure to MMS. However, MMS induces a variety of DNA lesions including base alkylation and generation of single- and double-strand breaks. Thus, we examined these cells after irradiation with UV light that generates a specific lesion, thymine dimers. We also examined the sensitivity of these cells to x rays because x rays and MMS are reported to induce double-strand breaks. As shown in Fig. 5 A (a), *xrcc3/blm+hXRCC3* cells were as sensitive to x rays as *xrcc3+hXRCC3* cells. The sensitivity of *xrcc3/blm* cells to x rays was not higher than that of either single mutant. Note that the x-ray sensitivity of *xrcc3* cells was very mild compared with that of *atm* cells, which are sensitive to ionizing radiation (Takao et al., 1999). Similar results were previously reported with *xrcc3* DT40 cells (Takata et al., 2001; Yonetani et al., 2005). However, hamster irsSF cells carrying a mutation in *XRCC3* are reportedly sensitive to ionizing radiation (Liu et al., 1998; Hinz, et al., 2005). The relatively high rate of recombination in DT40 cells may account for this inconsistency.

In contrast to their ionizing radiation sensitivity, *xrcc3/blm+hXRCC3* cells were mildly UV sensitive compared with *xrcc3+hXRCC3* cells, and this sensitivity was suppressed by deletion of *hXRCC3* to the level of *xrcc3* cells (Fig. 5 A, b). Chromosomal aberrations increased gradually during incubation after UV irradiation (Fig. 5 B, a). Details of various types of chromosome aberration are shown in Fig. S2 C. Chiasmata began to appear 6 h after UV irradiation and their frequency increased thereafter (Fig. 5 B, b). This type of chromosomal aberration was increased in *blm* cells. Deletion of *hXRCC3* suppressed various types of chromosome aberrations in *xrcc3/blm+hXRCC3* cells to the level seen in *xrcc3* cells. This especially concerned chromosome-type aberrations that manifest gaps or breaks at the same positions on sister chromatids (Figs. 5 C [a] and S2 D). The induction of mitotic chiasmata by UV irradiation in *xrcc3/blm+hXRCC3* and *xrcc3+hXRCC3* cells was almost completely suppressed by deletion of *hXRCC3* (Fig. 5 C, b).

Discussion

Cells derived from BS patients exhibit elevated levels of SCE, interchange between homologous chromosomes, and sensitivity to several DNA-damaging agents. In this paper, we performed a systematic genetic analysis of mutant chicken DT40 cells to explore the function of BLM and identify a putative mechanism underlying the phenotype of BS cells.

We demonstrated that *XRCC3* and *RAD54* are required for the elevated levels of SCE and MMS- or UV-induced mitotic

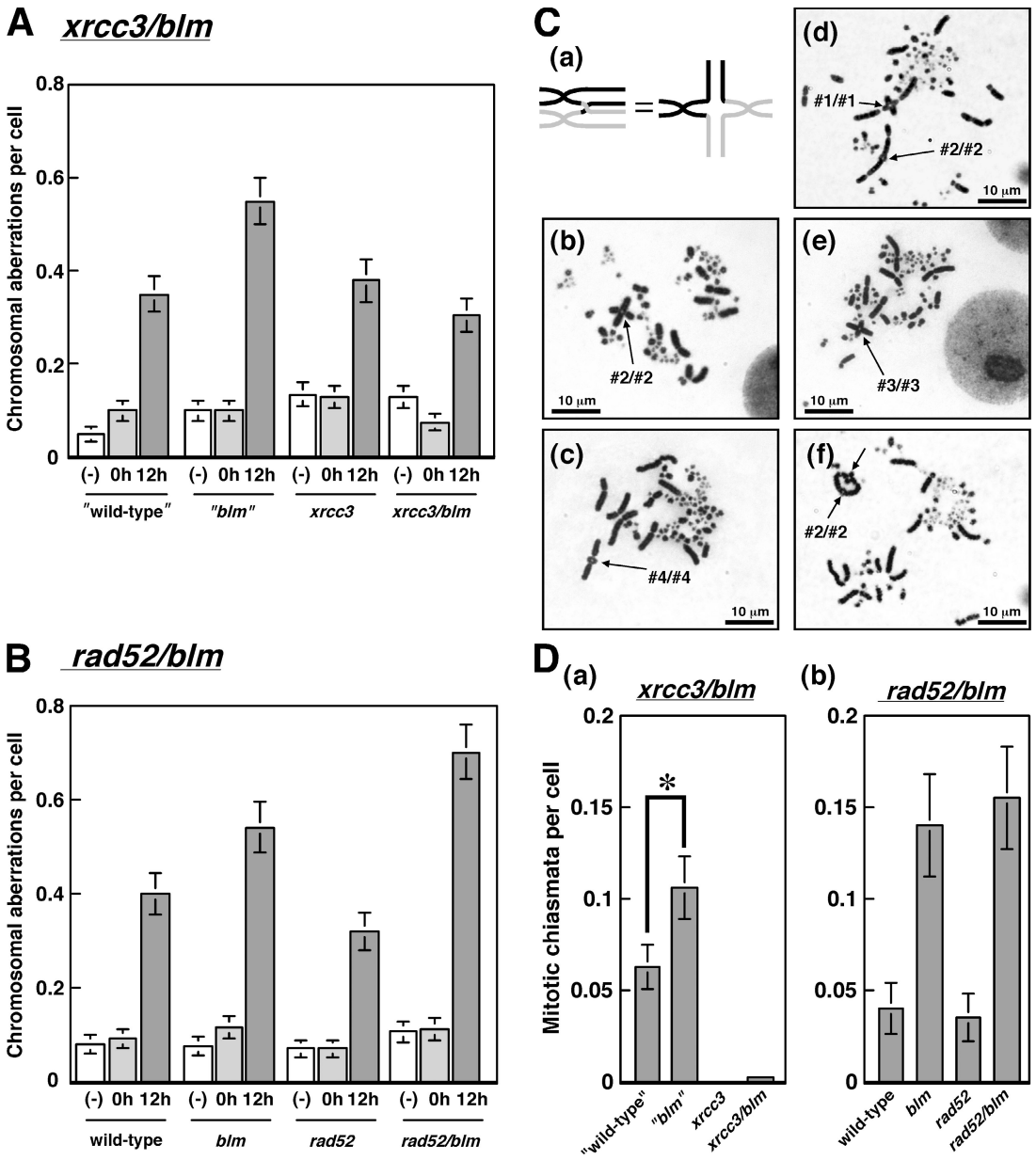

Figure 4. **MMS-induced chromosomal aberrations in mutant cells.** (A and B) Chromosomal aberrations. Cells were cultured in the presence of 8×10^{-6} (vol/vol) MMS for 4 h and transferred to fresh medium without MMS. Cells were harvested at the indicated times, and 200 cells in the first metaphase were analyzed for chromosomal aberrations, as described in Materials and methods. (−) indicates spontaneous chromosomal aberrations. Data represents SEM. (A) *xrcc3+hXRCC3* ("wild-type"), *xrcc3/blm+hXRCC3* ("*blm*"), *xrcc3*, and *xrcc3/blm* cells. (B) Wild-type, *blm*, *rad52*, and *rad52/blm* cells. (C and D) MMS-induced mitotic chiasmata. Cells were treated as described in A and B. (C) Images of MMS-induced mitotic chiasma in cells 12 h after exposure to MMS. (a) Schematic of a mitotic chiasma. (b–f) Typical examples of mitotic chiasmata resulting from recombination between homologous chromosomes. The point of recombination between homologous chromosomes is indicated with an arrow. The numbers in the figures indicate the number of macrochromosomes. (D) 400 (a) and 200 (b) cells in the first metaphase 12 h after MMS exposure were analyzed. Data represents SEM. (a) *xrcc3+hXRCC3*, *xrcc3/blm+hXRCC3*, *xrcc3*, and *xrcc3/blm* cells. There was a statistically significant difference between *xrcc3+hXRCC3* and *xrcc3/blm+hXRCC3* cells (*t* test; *, $P < 0.05$). (b) Wild-type, *blm*, *rad52*, and *rad52/blm* cells.

chiasmata observed in *blm* cells. The MMS sensitivity of *blm* cells was partially suppressed by disruption of *XRCC3*, but not by disruption of *RAD52*, *RAD*54, *WRN*, *RAD*18, or *KU*70. The suppression of *blm*-associated phenotypes upon disruption of *XRCC3*, particularly cell viability and increased chromosomal aberrations, was clearly evident in response to UV irradiation. Thus, the increased frequency of SCE, the sensitivities to MMS and UV, and the elevated frequency of mitotic chiasmata are caused by the function of XRCC3.

BLM and TOP3α negatively regulate the formation of SCE by acting on substrates generated by XRCC3

It is noteworthy that BLM interacts with RAD51D as well as RAD51 (Wu et al., 2001; Braybrooke et al., 2003). To determine the relationship between BLM and RAD51 in SCE formation, we constructed *rad51/blm+hRAD51* cells carrying a tetracycline-repressible human *RAD51* gene. Because *RAD51* is essential for cell viability, we could not assay the sensitivity of *rad51/blm*

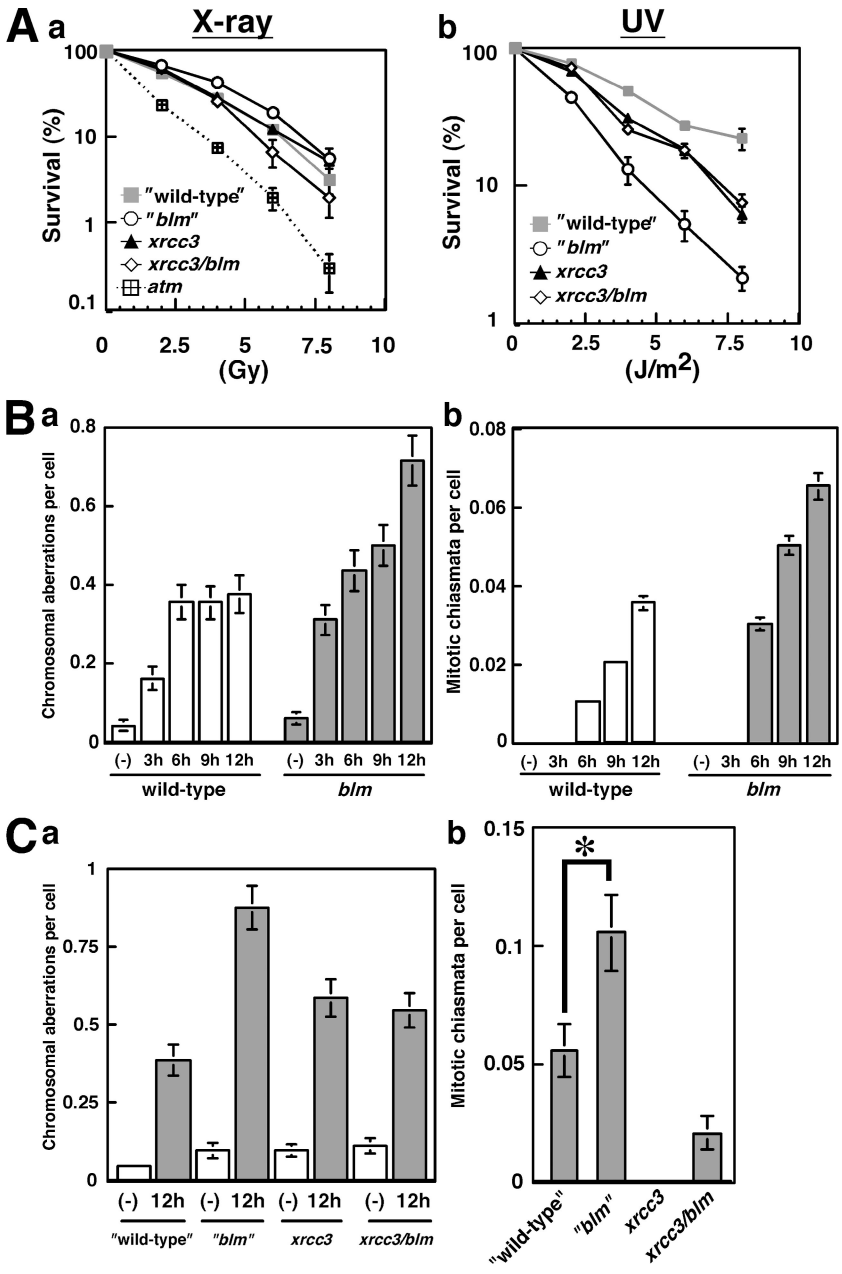

Figure 5. **Suppression of UV sensitivity and UV-induced chromosomal aberrations in *blm* cells by disruption of *XRCC3*.** (A) X-ray and UV sensitivities of *xrcc3+hXRCC3* ("wild-type"), *xrcc3/blm+hXRCC3* ("*blm*"), *xrcc3*, *xrcc3/blm*, and *atm* cells (Takao et al., 1999). Cells were irradiated with the indicated dose of x ray or UV. Colonies were counted after 10 d, and the percent survival was determined relative to the number of colonies derived from untreated cells. Representative data are shown. The error bars indicate SD. The differences in the duplicated data were often so minute that the SD were hidden by the symbols in the figures. X-ray (a) and UV survival curves (b) are shown. (B) UV-induced chromosomal aberrations (a) and mitotic chiasmata (b) in wild-type and *blm* cells. Samples were prepared every 3 h after irradiation with 8 J/m^2 UV. 200 cells in the first metaphase after UV irradiation were analyzed. Data represents the SEM. (C) UV-induced chromosomal aberrations (a) and mitotic chiasmata (b) in *xrcc3+hXRCC3*, *xrcc3/blm+hXRCC3*, *xrcc3*, and *xrcc3/blm* cells. Samples were prepared 12 h after irradiation with 8 J/m^2 of UV. 200 (a) and 400 (b) cells in the first metaphase were analyzed. (−) indicates spontaneous chromosomal aberrations. Data represents the SEM. There was a statistically significant difference between *xrcc3+hXRCC3* and *xrcc3/blm+hXRCC3* cells (*t* test; *, $P < 0.05$).

cells to DNA-damaging agents. We measured spontaneous SCE frequency under conditions of reduced hRAD51 expression. Under these conditions, we found that the elevated SCE frequency in *blm* cells was reduced considerably (Seki et al., 2006b). Next, to examine whether RAD51D functions like XRCC3, we generated *rad51d/blm* cells and found that, like XRCC3, RAD51D is required for the increased SCE frequency in *blm* cells (Fig. S4, available at http://www.jcb.org/cgi/content/full/jcb.200702183/DC1).

Biochemical studies of BLM showed that it has DNA helicase and branch migration activities. More importantly, it has been reported that BLM and TOP3α can dissolve double HJs to form noncrossover products in vitro (Wu and Hickson, 2003). Thus, it is possible that double HJs are formed as a result of the ability of XRCC3, RAD51D, RAD51, and RAD54 to deal with lesions and that these structures are dissolved by BLM and TOP3α in a manner that does not result in crossovers (Fig. S5, available at http://www.jcb.org/cgi/content/full/jcb.200702183/DC1). Therefore, defects in BLM, TOP3α, or both cause an increase in crossing over when HJs are resolved by certain nucleases, resulting in an increase in SCE.

A possible mechanism for the increase of mitotic chiasmata in *blm* cells after exposure to MMS or UV

Mitotic chiasmata are the visual manifestation of crossover recombination involving homologous chromosomes (Fig. S3 B). The increase of mitotic chiasmata in *blm* cells seems to be caused by a defect in a function of BLM/TOP3α that resolves recombination intermediates and prevents their crossing over. However, it is also possible that the increased incidence of mitotic chiasmata in *blm* cells is caused by an increase in lesions leading to homologous recombination, because the elevated

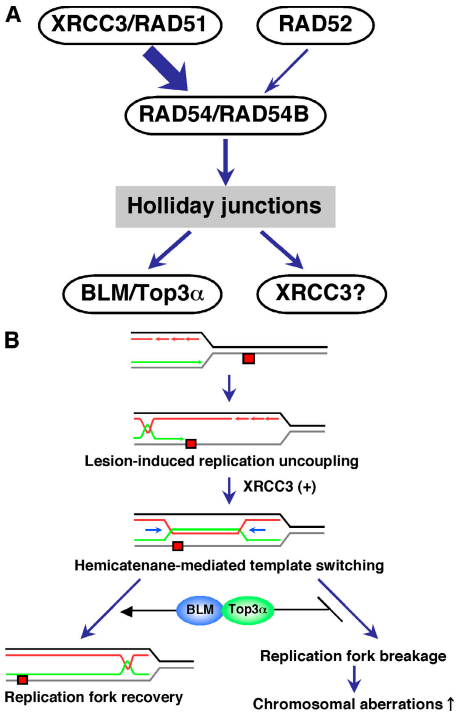

Figure 6. **Model of a role for BLM in the XRCC3-related damage tolerance pathway.** (A) A model based on canonical recombination pathways. (B) A model for a damage tolerance pathway involving XRCC3 and BLM based on the *S. cerevisiae* model proposed by Liberi et al. (2005) and Branzei et al. (2006).

level of mitotic chiasmata is very close to the elevated level of chromosomal aberrations.

The classical symmetrical quadriradial chromosomes often observed in human BS cells are identical to the mitotic chiasmata observed in the current study. A mitotic chiasma is a product of homologous recombination between homologous chromosomes. In fact, crossover recombination events involving homologous chromosomes have been observed in BS cells that carry different mutations in the two alleles of *BLM*, as indicated by the appearance of the wild-type *BLM* gene during cell culture (Ellis et al., 1995). The recombination between homologous chromosomes associated with crossovers may cause a loss of heterozygosity, which may underlie the predisposition to cancer observed in BS patients.

A possible mechanism for the suppression of the MMS and UV sensitivity of *blm* cells by disruption of *XRCC3*

In a previous paper, we demonstrated that *blm/rad54* double mutant cells are more sensitive to MMS than either of the corresponding single mutants (Fig. 3; W. Wang et al., 2000). XRCC3, RAD51B/C/D, and XRCC2 are RAD51 paralogues. In this paper, we found that disruption of *XRCC3* but not *RAD51D* (Fig. S4) suppresses the sensitivity of *blm* cells to both MMS and UV irradiation, suggesting that BLM functions downstream of XRCC3. However, *XRCC3* disruption exerted only a partial effect on MMS sensitivity, indicating that BLM also functions in an XRCC3-independent pathway. It is noteworthy that XRCC3 and RAD51D play similar but independent roles in the response to DNA damage (Yonetani et al., 2005). Thus, the discrepancy between the effects of the *XRCC3* deletion and the *RAD51D* deletion on the DNA damage sensitivity of *blm* cells could be caused by certain differences derived from these independent roles.

Mutant *xrcc3/rad54* cells showed higher sensitivity to MMS than either of the corresponding single mutants. One possible model that could explain the data is shown in Fig. 6 A. RAD51-mediated homologous recombination is probably initiated by many homologous recombination-related proteins and RAD51 paralogues, including XRCC3. The functions of the RAD51 paralogues could be supported by the RAD52 backup system (Fujimori et al. 2001), and the search and invasion of homologous regions by the DNA associated with RAD51 filaments could be supported by RAD54/RAD54B. HJs could be dissolved by BLM/TOP3α to avoid the formation of crossovers. As XRCC3 reportedly resolves HJs, it seems possible that XRCC3 would also function in the resolution of HJs (Liu et al., 2004) with the formation of crossovers. Accordingly, in the absence of BLM/TOP3α, XRCC3 would resolve HJs, resulting in increased SCE. This conjecture is supported by the observation that no high incidence of SCE is observed in *blm*/xrcc3 cells in the absence of both BLM and XRCC3. The higher sensitivity of the *blm/rad54* and *xrcc3/rad54* cells to MMS and UV compared with that of each mutant alone could be also explained by this model, assuming that RAD54B acts as a backup system in these circumstances. In addition, the suppression of the high SCE frequency and increased sensitivities of *blm* cells to MMS and UV by the *XRCC3* disruption could also be explained by this model if XRCC3 functions upstream of BLM. However, this model does not necessarily explain all the data obtained in this study.

However, there is another explanation for the suppression of SCE and *blm* cell sensitivity to DNA-damaging agents by the *XRCC3* disruption. Specific DNA damage produced by defects in BLM/TOP3α could require XRCC3 to initiate unnecessary homologous recombination that could lead to increased sensitivity to DNA-damaging agents or an increase in SCE. If there were no such initiation, the recombination induced by the defect in XRCC3 wouldn't cause cells to die or produce SCE.

We prefer the alternative model shown in Fig. 6 B to explain the suppression of the sensitivity of *blm* cells to DNA-damaging agents by *XRCC3* disruption. Interestingly, in fission yeast, the deletion of the human *RAD51D* or *XRCC2* (another RAD51 paralogue) homologues *rdl1* or *rlp1* suppresses the UV and MMS sensitivity of an *rqh1* disruptant, the *S. pombe BLM* homologue deletion mutant (Martin et al., 2006). Moreover, it is noteworthy that mutation of *SGS1*, the budding yeast homologue of *BLM,* leads to RAD51-dependent accumulation of cruciform structures when replication forks encounter DNA lesions on the template strand (Liberi et al., 2005; Branzei et al., 2006). Based on this observation, a model has been proposed in which stalled or failed replication forks are converted by RAD51 to intermediates that possess a pseudo double HJ, which is subsequently dissolved by Sgs1 and Top3α to restore the replication fork. This model proposes a novel, error-free lesion bypass system. In the context of this model, our results suggest that XRCC3 is involved in the formation of pseudo double HJs, which are

Table I. **DT40 strains used in this study**

Genotype	Disrupted gene (selective marker)	Expression plasmid	Reference
blm	*BLM* (His/Bsr)		W. Wang et al., 2000
wrn	*WRN* (His/Bsr)		Imamura et al., 2002
rad52	*RAD52* (His/Bsr)		Yamaguchi-Iwai et al., 1998
ku70	*KU70* (His/Bsr)		Takata et al., 1998
rad18	*RAD18* (His/Hyg)		Yamashita et al., 2002
top3α	*TOP3α* (Neo/His)	FLAG-*mTOP3α*: Hyg	Seki et al., 2006a
top3β	*TOP3β* (Puro/Bsr)		Seki et al., 2006a
atm	*ATM* (Neo/Puro)		Takao et al., 1999
rad52/blm	*RAD52* (His/Bsr), *BLM* (Hyg/Puro)		This study
ku70/blm	*KU70* (His/Bsr), *BLM* (Hyg/Neo)		This study
rad18/blm	*RAD18* (His/Hyg), *BLM* (Bsr/Neo)		This study
top3α/blm	*TOP3α* (Neo/His), *BLM* (Puro/Bsr)	FLAG-*mTOP3α*: Hyg	Seki et al., 2006a
top3β/blm	*TOP3β* (Puro/Bsr), *BLM* (Neo/His)		Seki et al., 2006a
xrcc3+hXRCC3	*XRCC3* (His/Bsr)	*hXRCC3*: Neo	Ishiai et al., 2004
xrcc3	*XRCC3* (His/Bsr)		Ishiai et al., 2004
xrcc3/blm+hXRCC3	*XRCC3* (His/Bsr), *BLM* (Eco/Puro)	*hXRCC3*: Neo	This study
xrcc3/blm	*XRCC3* (His/Bsr), *BLM* (Eco/Puro)		This study
xrcc3/wrn+hXRCC3	*XRCC3* (His/Bsr), *WRN* (Eco/Puro)	*hXRCC3*: Neo	This study
xrcc3/wrn	*XRCC3* (His/Bsr), *WRN* (Eco/Puro)		This study
xrcc3/wrn/blm+hXRCC3	*XRCC3* (His/Bsr), *WRN* (Eco/Puro), *BLM* (Bleo/Hyg)	*hXRCC3*: Neo	This study
xrcc3/wrn/blm	*XRCC3* (His/Bsr), *WRN* (Eco/Puro), *BLM* (Bleo/Hyg)		This study
xrcc3/rad54+hXRCC3	*XRCC3* (His/Bsr), *RAD54* (Hyg/Puro)	*hXRCC3*: Neo	This study
xrcc3/rad54	*XRCC3* (His/Bsr), *RAD54* (Hyg/Puro)		This study
xrcc3/blm/rad54+hXRCC3	*XRCC3* (His/Bsr), *BLM* (Eco/Puro), *RAD54* (Hyg/Bleo)	*hXRCC3*: Neo	This study
xrcc3/blm/rad54	*XRCC3* (His/Bsr), *BLM* (Eco/Puro), *RAD54* (Hyg/Bleo)		This study

Bleo, bleomycin; Bsr, blasticidin; Eco, ecogpt; His, histidinol; Hyg, hygromycin; Neo, neomycin; Puro, puromycin.

dissolved by BLM and TOP3α, resulting in the restoration of replication forks (Fig. 6 B). The failure to dissolve pseudo double HJs in *blm* cells stabilizes these structures and results in DNA breaks, which manifest themselves as chromosomal aberrations. Disruption of *XRCC3* suppresses the formation of detrimental intermediates in the absence of normal BLM function, leading to suppression of MMS and UV sensitivity and decreased numbers of MMS- and UV-induced chromosomal aberrations. XRCC3, but not RAD54, is required for slowing replication fork progression after exposure to DNA-damaging agents, such as UV and cisplatin (Henry-Mowatt et al., 2003). Although the mechanism underlying this phenomenon has not been addressed, this model provides a putative explanation. Upon activation of the XRCC3/BLM-dependent error-free lesion bypass pathway, progression of the replication fork halts until the repair process is completed. In the absence of XRCC3, replication proceeds, bypassing DNA lesions and generating gaps, as observed in yeast cells. Remaining lesions are bypassed or repaired by translesion synthesis or other mechanisms (Lopes et al., 2006). Recently, it has been reported that the MMS and UV sensitivity of *rad18* cells is also suppressed by disruption of *XRCC3* (Szuts et al., 2006). Our results indicate that BLM and RAD18 function in a different pathway upon exposure to MMS (Fig. 3 A). Thus, elucidation of the relationship between the XRCC3–BLM and XRCC3–RAD18 pathways should provide a more comprehensive view of DNA lesion–avoidance systems involving XRCC3, BLM, and RAD18.

Materials and methods

Cell culture and DNA transfection

Cells were cultured in RPMI 1640 supplemented with 10% fetal bovine serum, 1% chicken serum (Sigma-Aldrich), and 100 μg kanamycin/ml at 39.5°C. For gene targeting, 10^7 DT40 cells were electroporated with 30 μg of linearized targeting constructs using a Gene Pulser apparatus (Bio-Rad Laboratories) at 550 V and 25 μF. Drug-resistant colonies were selected in 96-well plates. Genomic DNA was isolated from drug-resistant clones. Gene disruption was confirmed by RT-PCR.

For generating double or triple mutants of *xrcc3* with mutations in *BLM*, *WRN*, and/or *RAD54*, these genes were disrupted in conditional *xrcc3* cells as described in Fig. 1. After gene disruption, the *hXRCC3* expression cassette was excised by Cre recombinase activated by 4-hydroxytamoxifen (Ishiai et al., 2004). The *BLM* gene was also disrupted in *rad52*, *ku70*, and *rad18* cells. The cell strains used in this study are summarized in Table I.

RT-PCR analysis

Total RNA was isolated using TRIzol (Invitrogen) and converted to cDNA with SuperscriptIII (Invitrogen). A part of each gene was amplified with *Ex Taq* polymerase. Primers were used to amplify *hXRCC3* (sense, 5′-GATTTGGATCTACTGGACCTGAATCCCAG-3′; antisense, 5′-GAGCTGCGTCCGGCCAGCTCAGTGATG-3′), *BLM* (sense, 5′-ACCAGCGTGTGTCTCTGCTG-3′; antisense, 5′-CTACAGATTTTGGAAGGGAAGC-3′), *WRN* (sense, 5′-CAGTGGAAAGTGATACATTCTGTTTTAGAAGAC-3′; antisense, 5′-CACCTGCAATTATCACAGCACTCTTC-3′), *RAD54* (sense, 5′-CTGGCCAAGAGGAAGGCGGGCGGCGAGGA-3′; antisense, 5′-TTAGGGAATCCCTCGCTGCTCTTCATGGG-3′), *RAD52* (sense, 5′-CGGCTCATACCATGAAGATGTGGG-3′; antisense, 5′-CCTGTTACGAGTTGTCATCTGGTGACG-3′), *KU70* (sense, 5′-CCAGCAAAATTATTAGTAGTGACAAGGATCTG-3′; antisense, 5′-CTGCATATGGTAGGAAAATGATGTGGAAACC-3′), *RAD18* (sense, 5′-CCCATAACTATTGTTCCCTTTGCATACGG-3′; antisense, 5′-GGGATTTAGAGAATCACACTGAGCATTATACACGTGC-3′), and *RECQL1* (sense, 5′-ATGACAGCTGTGGAAGTGCTA-3′; antisense, 5′-TCAGTCAAGAACAACAGGTTGGTCATCTC-3′; as a control) by RT-PCR.

Measurement of spontaneous SCE

5×10^5 cells were cultured for two cycles in a medium containing 10 μM BrdU and pulsed with 0.1 μg/ml colcemid for 2 h. The cells were harvested and treated with 75 mM KCl for 12 min at room temperature and fixed with methanol-acetic acid (3:1) for 30 min. The cell suspension was dropped onto wet glass slides and air dried. The cells on the slides were incubated with 10 μg/ml Hoechst 33258 stain in phosphate buffer, pH 6.8, for 20 min and rinsed with McIlvaine solution (164 mM Na_2HPO_4 and 16 mM citric acid, pH 7.0). The cells were exposed to a black light (352 nm) at a distance of 1 cm for 30 min, incubated in 2× SSC (0.3 M NaCl and 0.03 M sodium citrate) at 58°C for 20 min, and stained with 3% Giemsa solution (Merck) for 25 min.

Measurement of sensitivity to MMS, UV, and x rays

To determine MMS sensitivity, 4×10^2 cells were inoculated into 60-mm dishes containing various concentrations of MMS in a medium supplemented with 1.5% (wt/vol) methylcellulose, 15% fetal bovine serum, and 1.5% chicken serum. For UV sensitivity, cells were suspended in 1 ml phosphate-buffered saline, inoculated into 6-well plates, and irradiated with various doses of UV. For x-ray sensitivity, cells were suspended in 1 ml phosphate-buffered saline, inoculated into 1.5-ml tubes, and irradiated with various x-ray doses. UV- or x-irradiated cells were inoculated into 60-mm dishes containing a medium supplemented with 1.5% (wt/vol) methylcellulose, 15% fetal bovine serum, and 1.5% chicken serum. Colonies were counted after 7–14 d, and the percent survival was determined relative to the number of colonies of untreated cells. We performed the same survival experiments several times (Fig. S1). After confirming that all the data gave similar results, we presented representative data (Fig. S1, surrounded by red square). In each experiment, we tested each cell genotype in duplicate.

Detection of chromosomal aberrations

Cells were treated with 0.1 μg/ml colcemid the last 2 h to increase metaphase-arrested cells and were harvested at the indicated time points. Harvested cells were treated with 75 mM KCl for 12 min at room temperature and fixed with methanol-acetic acid (3:1) for 30 min. The cell suspension was dropped onto wet glass slides, air dried, and stained with 3% Giemsa solution, pH 6.8, for 25 min, and the cells were examined by light microscopy.

To enumerate MMS- and UV-induced chromosomal aberrations, cells were cultured in the presence of 10 μM BrdU. Incorporation of BrdU into sister chromatids was used to discriminate first and second metaphase, and only chromosomal aberrations occurring during first metaphase were counted.

All images of mitotic chiasma were collected with a camera (CoolSNAP; Photometrics) mounted on a microscope (BX50F; Olympus). CoolSNAP version 1.2.0 (Roper Scientific) was used for image acquisition.

Online supplemental material

Fig. S1 shows survival curves of various mutant cells exposed to MMS. Fig. S2 shows the classification of chromosomal aberrations. Fig. S3 shows mitotic chiasma. Fig. S4 shows characterization of *rad51d/blm* cells. Fig. S5 is a schematic model of SCE formation. Online supplemental material is available at http://www.jcb.org/cgi/content/full/jcb.200702183/DC1.

This work was supported by grants-in-aid for scientific research on priority areas from the Ministry of Education, Culture, Sports, Science and Technology.

Submitted: 28 February 2007
Accepted: 6 September 2007

References

Bachrati, C.Z., and I.D. Hickson. 2003. RecQ helicases: suppressors of tumorigenesis and premature aging. *Biochem. J.* 374:577–606.

Bezzubova, O., A. Silbergleit, Y. Yamaguchi-Iwai, S. Takeda, and J.M. Buerstedde. 1997. Reduced X-ray resistance and homologous recombination frequencies in a *RAD54*$^{-/-}$ mutant of the chicken DT40 cell line. *Cell.* 89:185–193.

Branzei, D., J. Sollier, G. Liberi, X. Zhao, D. Maeda, M. Seki, T. Enomoto, K. Ohta, and M. Foiani. 2006. Ubc9- and mms21-mediated sumoylation counteracts recombinogenic events at damaged replication forks. *Cell.* 127:509–522.

Braybrooke, J.P., J.L. Li, L. Wu, F. Caple, F.E. Benson, and I.D. Hickson. 2003. Functional interaction between the Bloom's syndrome helicase and the RAD51 paralog, RAD51L3 (RAD51D). *J. Biol. Chem.* 278:48357–48366.

Chaganti, R.S., S. Schonberg, and J. German. 1974. A manyfold increase in sister chromatid exchanges in Bloom's syndrome lymphocytes. *Proc. Natl. Acad. Sci. USA*. 71:4508–4512.

Ellis, N.A., J. Groden, T.Z. Ye, J. Straughen, D.J. Lennon, S. Ciocci, M. Proytcheva, and J. German. 1995. The Bloom's syndrome gene product is homologous to RecQ helicases. *Cell*. 83:655–666.

Fujimori, A., S. Tachiiri, E. Sonoda, L.H. Thompson, P.K. Dhar, M. Hiraoka, S. Takeda, Y. Zhang, M. Reth, and M. Takata. 2001. Rad52 partially substitutes for the Rad51 paralog XRCC3 in maintaining chromosomal integrity in vertebrate cells. *EMBO J.* 20:5513–5520.

Gangloff, S., J.P. McDonald, C. Bendixen, L. Arthur, and R. Rothstein. 1994. The yeast type I topoisomerase Top3 interacts with Sgs1, a DNA helicase homolog: a potential eukaryotic reverse gyrase. *Mol. Cell. Biol.* 14:8391–8398.

German, J. 1993. Bloom syndrome: a mendelian prototype of somatic mutational disease. *Medicine*. 72:393–406.

Henry-Mowatt, J., D. Jackson, J.Y. Masson, P.A. Johnson, P.M. Clements, F.E. Benson, L.H. Thompson, S. Takeda, S.C. West, and K.W. Caldecott. 2003. XRCC3 and Rad51 modulate replication fork progression on damaged vertebrate chromosomes. *Mol. Cell*. 11:1109–1117.

Hinz, J.M., N.A. Yamada, E.P. Salazar, R.S. Tebbs, and L.H. Thompson. 2005. Influence of double-strand-break repair pathways on radiosensitivity throughout the cell cycle in CHO cells. *DNA Repair (Amst.)*. 4:782–792.

Huttner, K.M., and F.H. Ruddle. 1976. Study of mitomycin C-induced chromosomal exchange. *Chromosoma*. 56:1–13.

Imamura, O., K. Fujita, C. Itoh, S. Takeda, Y. Furuichi, and T. Matsumoto. 2002. Werner and Bloom helicases are involved in DNA repair in a complementary fashion. *Oncogene*. 21:954–963.

Ira, G., A. Malkova, G. Liberi, M. Foiani, and J.E. Haber. 2003. Srs2 and Sgs1-Top3 suppress crossovers during double-strand break repair in yeast. *Cell*. 115:401–411.

Ishiai, M., M. Kimura, K. Namikoshi, M. Yamazoe, K. Yamamoto, H. Arakawa, K. Agematsu, N. Matsushita, S. Takeda, J.M. Buerstedde, and M. Takata. 2004. DNA cross-link repair protein SNM1A interacts with PIAS1 in nuclear focus formation. *Mol. Cell. Biol.* 24:10733–10741.

Kitao, S., A. Shimamoto, M. Goto, R.W. Miller, W.A. Smithson, N.M. Lindor, and Y. Furuichi. 1999. Mutations in RECQL4 cause a subset of cases of Rothmund-Thomson syndrome. *Nat. Genet.* 22:82–84.

Liberi, G., G. Maffioletti, C. Lucca, I. Chiolo, A. Baryshnikova, C. Cotta-Ramusino, M. Lopes, A. Pellicioli, J.E. Haber, and M. Foiani. 2005. Rad51-dependent DNA structures accumulate at damaged replication forks in *sgs1* mutants defective in the yeast ortholog of BLM RecQ helicase. *Genes Dev.* 19:339–350.

Liu, N., J.E. Lamerdin, R.S. Tebbs, D. Schild, J.D. Tucker, M.R. Shen, K.W. Brookman, M.J. Siciliano, C.A. Walter, W. Fan, et al. 1998. XRCC2 and XRCC3, new human Rad51-family members, promote chromosome stability and protect against DNA cross-links and other damages. *Mol. Cell*. 1:783–793.

Liu, Y., J.Y. Masson, R. Shah, P. O'Regan, and S.C. West. 2004. RAD51C is required for Holliday junction processing in mammalian cells. *Science*. 303:243–246.

Lopes, M., M. Foiani, and J.M. Sogo. 2006. Multiple mechanisms control chromosome integrity after replication fork uncoupling and restart at irreparable UV lesions. *Mol. Cell*. 21:15–27.

Martin, V., C. Chahwan, H. Gao, V. Blais, J. Wohlschlegel, J.R. Yates III, C.H. McGowan, and P. Russell. 2006. Sws1 is a conserved regulator of homologous recombination in eukaryotic cells. *EMBO J.* 25:2564–2574.

Meetei, A.R., S. Sechi, M. Wallisch, D. Yang, M.K. Young, H. Joenje, M.E. Hoatlin, and W. Wang. 2003. A multiprotein nuclear complex connects Fanconi anemia and Bloom syndrome. *Mol. Cell. Biol.* 23:3417–3426.

Raynard, S., W. Bussen, and P. Sung. 2006. A double Holliday junction dissolvasome comprising BLM, topoisomerase IIIα, and BLAP75. *J. Biol. Chem.* 281:13861–13864.

Seki, M., T. Nakagawa, T. Seki, G. Kato, S. Tada, Y. Takahashi, A. Yoshimura, T. Kobayashi, A. Aoki, M. Otsuki, et al. 2006a. Bloom helicase and DNA topoisomerase IIIα are involved in the dissolution of sister chromatids. *Mol. Cell. Biol.* 26:6299–6307.

Seki, M., S. Tada, and T. Enomoto. 2006b. Function of recQ family helicase in genome stability. *Subcell. Biochem.* 40:49–73.

Stewart, E., C.R. Chapman, F. Al-Khodairy, A.M. Carr, and T. Enoch. 1997. *rqh1+*, a fission yeast gene related to the Bloom's and Werner's syndrome genes, is required for reversible S phase arrest. *EMBO J.* 16:2682–2692.

Sung, P., K.M. Trujillo, and S. Van Komen. 2000. Recombination factors of *Saccharomyces cerevisiae*. *Mutat. Res.* 451:257–275.

Szuts, D., L.J. Simpson, S. Kabani, M. Yamazoe, and J.E. Sale. 2006. A role for RAD18 in homologous recombination in DT40. *Mol. Cell. Biol.* 26:8032–8041.

Takao, N., H. Kato, R. Mori, C. Morrison, E. Sonada, X. Sun, H. Shimizu, K. Yoshioka, S. Takeda, and K. Yamamoto. 1999. Disruption of ATM in p53-null cells causes multiple functional abnormalities in cellular response to ionizing radiation. *Oncogene*. 18:7002–7009.

Takata, M., M.S. Sasaki, E. Sonoda, C. Morrison, M. Hashimoto, H. Utsumi, Y. Yamaguchi-Iwai, A. Shinohara, and S. Takeda. 1998. Homologous recombination and non-homologous end-joining pathways of DNA double-strand break repair have overlapping roles in the maintenance of chromosomal integrity in vertebrate cells. *EMBO J.* 17:5497–5508.

Takata, M., M.S. Sasaki, S. Tachiiri, T. Fukushima, E. Sonoda, D. Schild, L.H. Thompson, and S. Takeda. 2001. Chromosome instability and defective recombinational repair in knockout mutants of the five Rad51 paralogs. *Mol. Cell. Biol.* 21:2858–2866.

Therman, E., and E.M. Kuhn. 1981. Mitotic crossing-over and segregation in man. *Hum. Genet.* 59:93–100.

von Kobbe, C., P. Karmakar, L. Dawut, P. Opresko, X. Zeng, R.M. Brosh Jr., I.D. Hickson, and V.A. Bohr. 2002. Colocalization, physical, and functional interaction between Werner and Bloom syndrome proteins. *J. Biol. Chem.* 277:22035–22044.

Wang, W., M. Seki, Y. Narita, E. Sonoda, S. Takeda, K. Yamada, T. Masuko, T. Katada, and T. Enomoto. 2000. Possible association of BLM in decreasing DNA double strand breaks during DNA replication. *EMBO J.* 19:3428–3435.

Wang, Y., D. Cortez, P. Yazdi, N. Neff, S.J. Elledge, and J. Qin. 2000. BASC, a super complex of BRCA1-associated proteins involved in the recognition and repair of aberrant DNA structures. *Genes Dev.* 14:927–939.

Wu, L., and I.D. Hickson. 2003. The Bloom's syndrome helicase suppresses crossing over during homologous recombination. *Nature*. 426:870–874.

Wu, L., S.L. Davies, N.C. Levitt, and I.D. Hickson. 2001. Potential role for the BLM helicase in recombinational repair via a conserved interaction with RAD51. *J. Biol. Chem.* 276:19375–19381.

Wu, L., C.Z. Bachrati, J. Ou, C. Xu, J. Yin, M. Chang, W. Wang, L. Li, G.W. Brown, and I.D. Hickson. 2006. BLAP75/RMI1 promotes the BLM-dependent dissolution of homologous recombination intermediates. *Proc. Natl. Acad. Sci. USA*. 103:4068–4073.

Yamaguchi-Iwai, Y., E. Sonoda, J.M. Buerstedde, O. Bezzubova, C. Morrison, M. Takata, A. Shinohara, and S. Takeda. 1998. Homologous recombination, but not DNA repair, is reduced in vertebrate cells deficient in RAD52. *Mol. Cell. Biol.* 18:6430–6435.

Yamashita, Y.M., T. Okada, T. Matsusaka, E. Sonoda, G.Y. Zhao, K. Araki, S. Tateishi, M. Yamaizumi, and S. Takeda. 2002. RAD18 and RAD54 cooperatively contribute to maintenance of genomic stability in vertebrate cells. *EMBO J.* 21:5558–5566.

Yin, J., A. Sobeck, C. Xu, A.R. Meetei, M. Hoatlin, L. Li, and W. Wang. 2005. BLAP75, an essential component of Bloom's syndrome protein complexes that maintain genome integrity. *EMBO J.* 24:1465–1476.

Yonetani, Y., H. Hochegger, E. Sonoda, S. Shinya, H. Yoshikawa, S. Takeda, and M. Yamazoe. 2005. Differential and collaborative actions of Rad51 paralog proteins in cellular response to DNA damage. *Nucleic Acids Res.* 33:4544–4552.

Yu, C.E., J. Oshima, Y.H. Fu, E.M. Wijsman, F. Hisama, R. Alisch, S. Matthews, J. Nakura, T. Miki, S. Ouais, and G.M. Martin. 1996. Positional cloning of the Werner's syndrome gene. *Science*. 272:258–262.